Physics of the Solid State, 2023, Vol. 65, No. 8

12,13

The effect of heat treatment on the structure and electrochemical characteristics of composite based on multi-walled carbon nanotubes and manganese oxide

© S.N. Nesov[1,2], Yu.A. Sten'kin[2], P.M. Korusenko[1,3], V.V. Bolotov[1,2], S.A. Matyushenko[1,2]

[1] Omsk State Technical University,
Omsk, Russia
[2] Omsk Scientific Center, Siberian Branch, Russian Academy of Sciences,
Omsk, Russia
[3] St. Petersburg State University,
St. Petersburg, Russia
E-mail: nesov55@mail.ru

Received June 30, 2023
Revised June 30, 2023
Accepted July 5, 2023

In this paper, the effect of heat treatment in an inert medium on the structure and electrochemical characteristics of a composite based on multi-walled carbon nanotubes (MWCNTs) and manganese oxide formed by deposition from a $KMnO_4$ solution is investigated. As a result of heat treatment composite (500°C) in argon on the surface of multi-walled carbon nanotubes are formed nanoparticles of non-stoichiometric manganese oxide. X-ray photoelectron spectroscopy data indicate a high degree of functionalization of the surface of carbon nanotubes by oxygen-containing groups, as well as the possible formation chemical bonds at the interfaces of the composite. Electrochemical measurements showed that the specific capacity of the composite after heat treatment ($\sim 88-50$ F/g) exceeds the capacity of the original MWCNTs ($18-15$ F/g) in the current range discharge $0.1-1$ A/g.

Keywords: supercapacitors, 1D-structure, hydrothermal decomposition, charge-discharge characteristics.

DOI: 10.61011/PSS.2023.08.56588.135

1. Introduction

The development of new materials for highly efficient chemical current sources is an urgent task of modern materials science. Supercapacitors, which are characterized by short charge times and high values of specific power, capacitance and cyclic stability are among the promising devices. Supercapacitors are increasingly being used in microelectronics, power supply of electric transport engines, systems that stabilize the operation of high-voltage power transmission systems, as well as pre-starting devices of engines operating at low temperatures [1]. Various types of carbon having a high specific surface area and a low electrical resistance value as a rule are used as a basis for the manufacture of electrodes of such devices [1,2].

Multi-walled carbon nanotubes (MWCNT) have high electrical conductivity, and their 1D frame structure can also provide high mechanical characteristics of supercapacitor electrodes. This opens up the possibility of obtaining materials based on MWCNT for supercapacitors with variable geometry (flexible devices), and also reduces the number of binding polymers in the production of electrodes that negatively affect the electrical conductivity of [3]. However, MWCNT do not have record high values of specific surface area ($\sim 10-500\,m^2/g$ [4]) among other carbon materials, therefore they have relatively low values of specific capacity. It is possible to increase the capacitance characteristics of MWCNT by decorating their surface with electrochemically active metal oxides (RuO_2, MnO_2, NiO, etc.) [5]. Such oxides provide additional capacity of the material due to the course of reversible oxidation-reduction reactions (RORR) when interacting with electrolytes. Manganese oxide has a high theoretical value of specific capacity (more than 1370 F/g) and at the same time is an affordable and non-toxic material [6,7]. However, the use of manganese oxide „in its pure form" is limited by insufficient electrical conductivity and the tendency of its individual particles to agglomerate during operation of the supercapacitor, which leads to a decrease in the surface area available for the electrolyte and degradation of the functional characteristics of the material [8].

This paper studies the effect of heat treatment in an inert atmosphere on the structure and electrochemical characteristics of a composite based on MWCNT and manganese oxide formed by hydrothermal decomposition of potassium permanganate using scanning electron microscopy (SEM), X-ray photoelectron spectroscopy (XPS), galvanostatic charge−discharge and cyclic volt-amperometry (CV) ($KMnO_4$).

2. Experiment

Commercial multi-walled carbon nanotubes were used to form the MWCNT|MnO_x composite (produced by BIC SB

RAS, Russia, Novosibirsk). MWCNT were synthesized by chemical vapor deposition (CVD) using to the procedure specified in [9,10]. MWCNT diameter ~ 10 nm, specific surface area $\sim 360\,\mathrm{m^2/g}$. MWCNTs was treated in an aqueous solution of nitric acid for 5 min, followed by washing in distilled water to increase hydrophilic capacity. Then the MWCNT was mixed with powder $KMnO_4$ in a mass ratio of 8 : 2 and distilled water was added. The resulting solution was kept at room temperature and atmospheric pressure with constant stirring 72 h. Then the composite was washed with distilled water and dried at a pressure of ~ 1 Pa and a temperature of 80°C for 10 h. Further, a part of the resulting composite was annealed at a temperature of 500°C in an argon atmosphere in order to optimize the structure and composition of the composite.

Carl Zeiss AURIGA scanning electron microscope (St. Petersburg State University, St. Petersburg, Russia) was used to analyze the structure of the initial MWCNT and the composite before and after heat treatment. The accelerating voltage during recording of SEM images was 10 kV. The chemical state of the composite was analyzed using X-ray photoelectron spectroscopy. A source with Al-K_α-radiation of the Surface Science Center equipment (OSC SB RAS, Russia, Omsk) was used to excite X-ray radiation. The XPS spectra were measured under ultrahigh vacuum conditions (pressure in the analysis chamber $\sim 10^{-7}$ Pa). The area of the X-ray beam was $\sim 3\,\mathrm{mm}^2$, the source power was 240 W. The energy resolution when registering the spectra of the core-level lines was ~ 0.2 eV, survey spectra ~ 1.2 eV. The effective depth of this method of analysis is ~ 5 nm.

Electrodes were prepared for the analysis of electrochemical characteristics on the basis of the studied materials 10 mass.%. of polymer binder (polyvinylendene fluoride) and organic solvent (N-methyl-2-pyrrolidone) were added to the active material (MWCNT or composites) for the prepration of electrodes, followed by prolonged stirring until a homogeneous viscous mass was formed. Further, the resulting mass was dried for 1 h at a temperature of 50° C, followed by rolling into plates with a thickness of no more than 100 μm, from which electrodes with a size of $10 \times 15\,\mathrm{mm}^2$ were cut. The resulting electrodes were dried for 24 h at a temperature of 80°C and a pressure of about 1 Pa to remove solvent residues. Electrodes based on MWCNT, as well as initial and annealed composites with manganese oxide (MWCNT|MnO_x and MWCNT|MnO_x_500, respectively) were prepared for a comparative analysis of electrochemical characteristics.

Electrochemical characteristics of composite samples were evaluated by cyclic volt-amperometry (CV), as well as galvanostatic charge-discharge using a potentiostat-galvanostat P-40X (Elins, Zelenograd, Russia). The measurements were carried out using a three-electrode cell. A platinum plate of size $10 \times 15\,\mathrm{mm}^2$ was used as an antielectrode. A standard Ag|AgCl|KCl electrode was used as a reference electrode, which was placed in an electrochemical cell using a Luggin capillary. A 1-M aqueous solution of Na_2SO_4 was used as the electrolyte. The specific capacitance (C_s) was calculated using the results of galvanostatic measurements as: $Cs = (I\Delta t)/(Um)$, where I — discharge current, Δt — discharge time, U — potential window (0.8 V), m — the mass of the active material in the electrode. Before taking measurements, the electrodes were kept in the electrolyte for 6 h, and then stabilized in the CV mode at a potential sweep rate of 20 mV/s (100 charge-discharge cycles).

3. Results and discussion

3.1. SEM data

Figure 1 shows SEM images of the original MWCNT and composite before and after heat treatment in an inert atmosphere. The outer diameter of the MWCNT

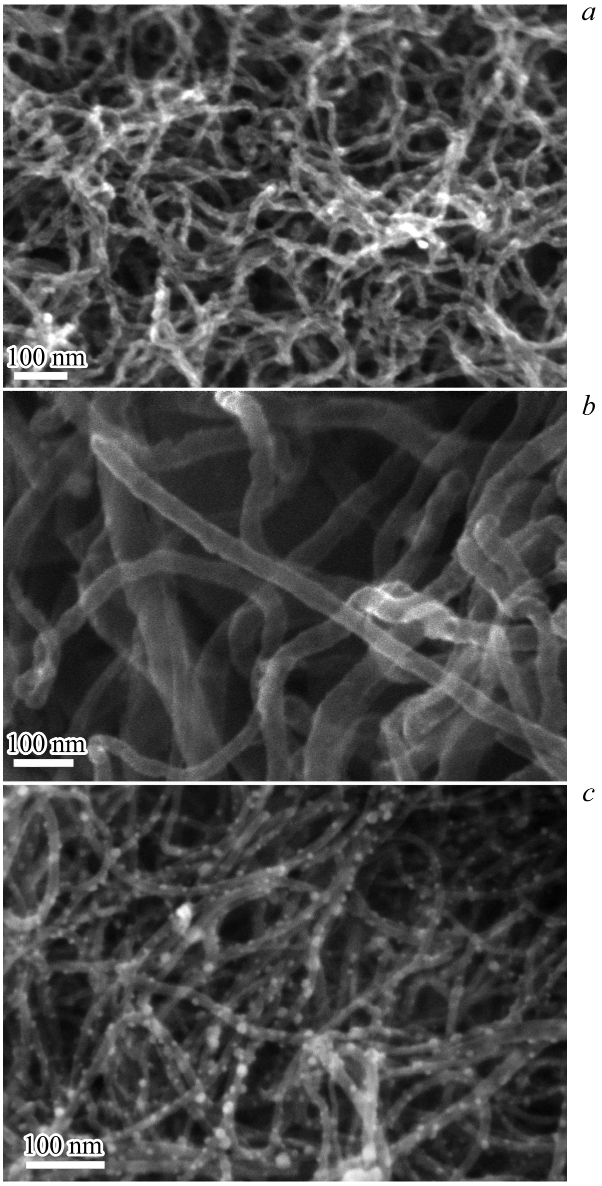

Figure 1. SEM images: *a*) initial MWCNT; *b*) composite MWCNT|MnO_x; *c*) MWCNT|MnO_x_500.

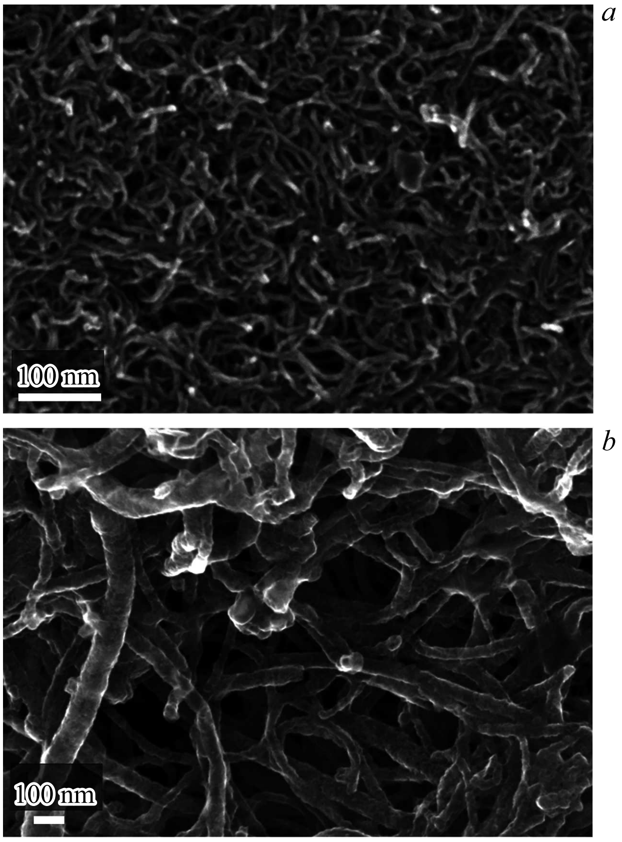

Figure 2. SEM images of the electrode surface: *a*) based on the initial MWCNT; *b*) based on the composite MWCNT|MnO$_x$.

(Figure 1,*a*) is ~ 10 nm. In the images of the initial composite (Figure 1,*b*), the diameter of the MWCNT is ~ 20–70 nm, which indicates the presence of a manganese oxide layer with a thickness of ~ 5–30 nm. MWCNT after deposition of manganese oxide do not stick together into agglomerates and retain a porous structure. Large agglomerates of manganese oxide are also observed quite rarely. The presence of a set of fairly evenly distributed individual nanoparticles, whose sizes range from several units to ~ 20 nm, is observed in the composite after heat treatment in an inert medium (Figure 1,*c*) on the surface of carbon nanotubes. At the same time, the external diameters of the MWCNT in areas where there are no manganese oxide nanoparticles (Figure 1,*c*) practically do not differ from the diameters of the initial carbon nanotubes (Figure 1,*a*).

Figure 2 shows SEM images of the surface of electrodes prepared on the basis of MWCNT and the composite MWCNT|MnO$_x$ for electrochemical measurements. It can be seen that the surface of the electrodes has a porous structure and has a fairly uniform distribution of the binder polymer.

The image with a high spatial resolution allows us to say that the MWCNT network forms a structure with pores, the sizes of which range from several hundred nanometers to units of micrometers.

Table 1. Element composition of samples according to XPS data

Sample	Concentration, at.%			
	C	O	Mn	K
MWCNT	98.5	1.5	–	–
MWCNT|MnO$_x$	53.9	36.7	7.9	1.5
MWCNT|MnO$_x$_500	62.7	31.6	4.8	0.9

3.2. XPS data

Figure 3 shows the survey XPS spectra of the studied materials. The results of the quantitative analysis performed using the method of elemental sensitivity coefficients are listed in Table 1.

An intense carbon peak (Figure 3, curve *1*) C1s and low-intensity oxygen peak O1s is observed in the MWCNT spectrum. Carbon peaks (Figure 3, curves *2* and *3*) C1s, oxygen O1s, manganese (Mn 2p, 3s, 3p), as well as potassium peaks (K2s, K2p) are observed in the spectra of composites. The presence of potassium is attributable to the residues of a small amount of the precursor of manganese oxide (potassium permanganate) in the samples.

According to the data in Table 1 the composite MWCNT|MnO$_x$ has an increased oxygen content, which indicates a significant oxidation of the surface of carbon nanotubes during the synthesis of the composite. A noticeable decrease in the concentration of manganese is observed in the MWCNT|MnO$_x$_500 composite. This is quite consistent with the results of the analysis of the morphology of composites by the SEM method. At the same time, the change in oxygen concentration is relatively small. This allows assuming the preservation of a significant part of the functional groups on the surface of the MWCNT after heat treatment in an inert environment. The amount of potassium is also reduced, which may be due to the partial removal of

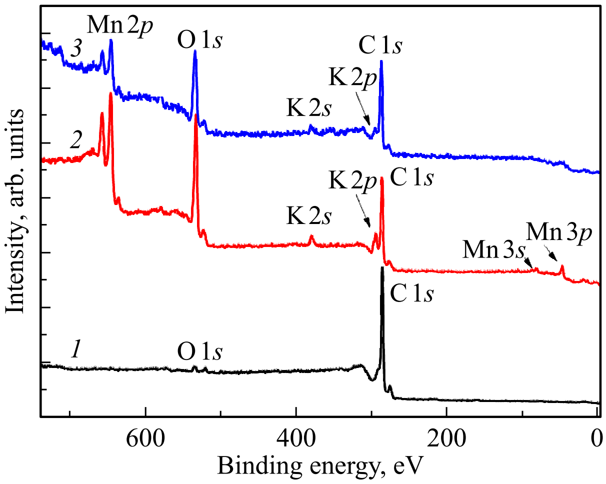

Figure 3. Survey XPS spectra: *1* — MWCNT; *2* — composite MWCNT|MnO$_x$; *3* — MWCNT|MnO$_x$_500.

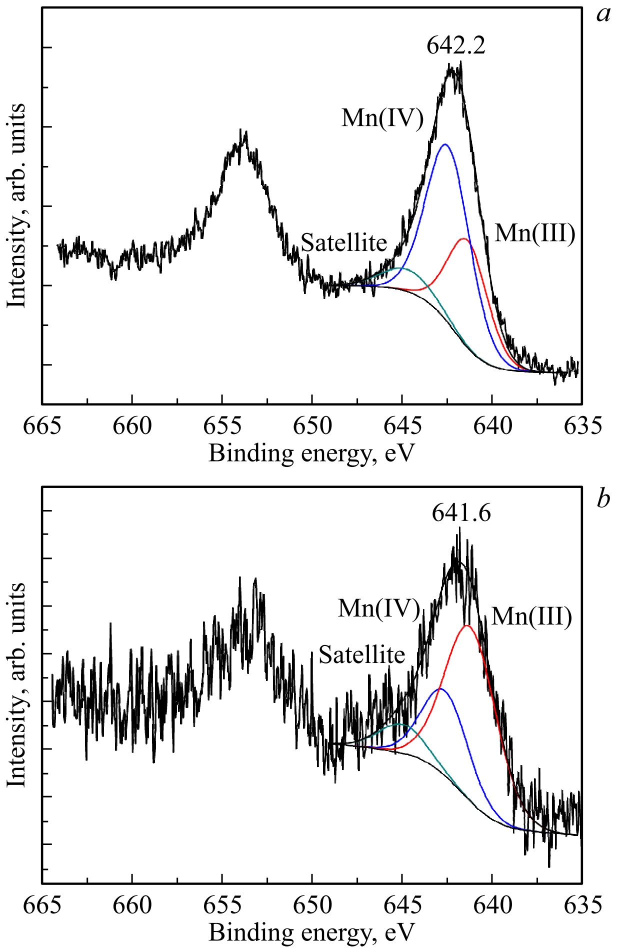

Figure 4. Mn2p XPS spectra: *a*) composite MWCNT|MnO$_x$; *b*) MWCNT|MnO$_x$_500.

potassium permanganate residues together with manganese oxide from the surface of the MWCNT.

The analysis of the chemical state of manganese was conducted using fitting of the XPS spectra of Mn2p$_{3/2}$ (Figure 4). The position of the maximum line in the spectrum of the composite after annealing shifts to the region of low binding energies (Figure 4, *b*) relative to the spectrum of the initial composite (Figure 4, *a*). The fitting results show that in both spectra there are states with maxima at binding energies 641.5 and 642.8 eV, corresponding to the oxides Mn(III) and Mn(IV) [11–13], and also a satellite at binding energies ~ 645 eV, characteristic of the XPS spectra of transition metals [11]. In the spectrum of the initial composite (Figure 4, *a*), Mn(IV) states prevail, whereas in the spectrum of the composite after heat treatment (Figure 4, *b*), the relative intensity of the component corresponding to the Mn oxide increases(III).

The XPS C1s spectra of the original MWCNT (Figure 5, *a*) were approximated using 5 components (C1–C5) corresponding to the carbon states in the composition of various functional oxygen-containing groups, as well as $\pi-\pi^*$ plasmon, present in the spectra of graphitized materials with a low degree of crystal structure imperfection. Components with bond energy maxima ~ 284.5 (C1), ~ 285.0 (C2), ~ 286.5 (C3), ~ 288.5 (C4) and 289.5 eV respond carbon states in the composition C=C(sp^2), C–C(sp^3)/C*–C(O), C–O/C–O–C, C=O and COOH respectively [14–16]. The total relative proportion of components corresponding to carbon-carbon bonds (components C1 and C2), is more than 94%.

The intensity of the components of C3–C5 increases markedly in the C1s spectrum of the composite MWCNT|MnO$_x$ (Figure 5, *b*). The value of the full width

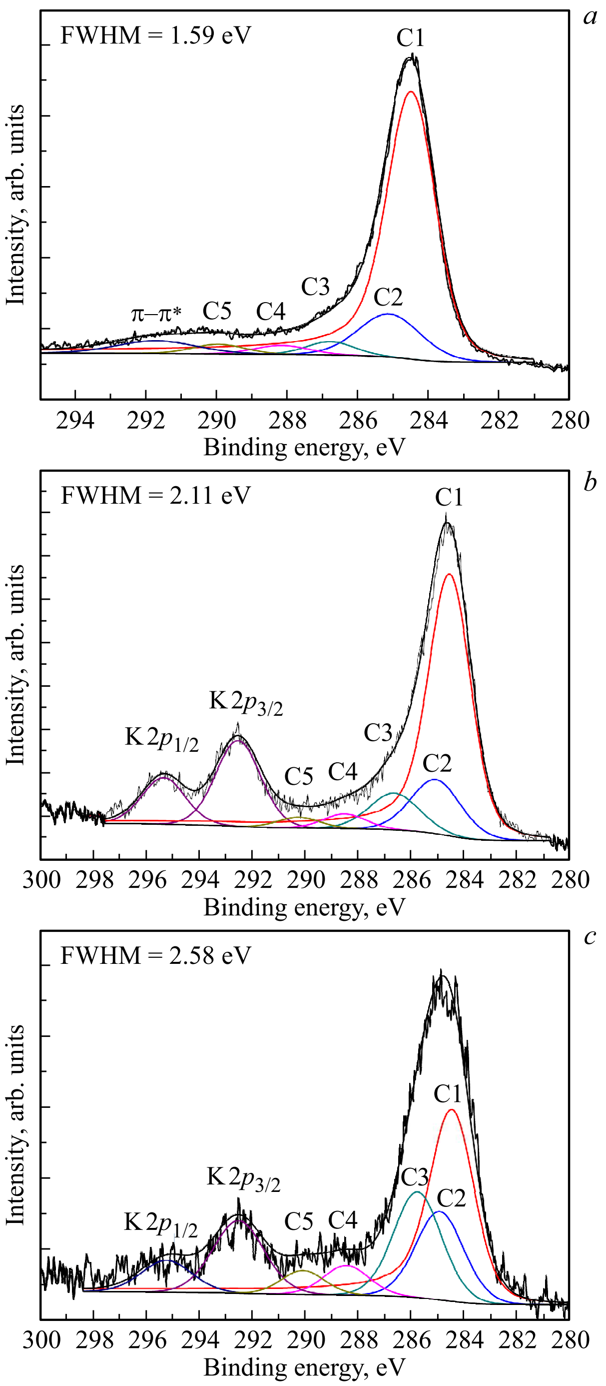

Figure 5. XPS spectra of C1s: *a*) original MWCNT; *b*) composite MWCNT|MnO$_x$; *c*) MWCNT|MnO$_x$_580.

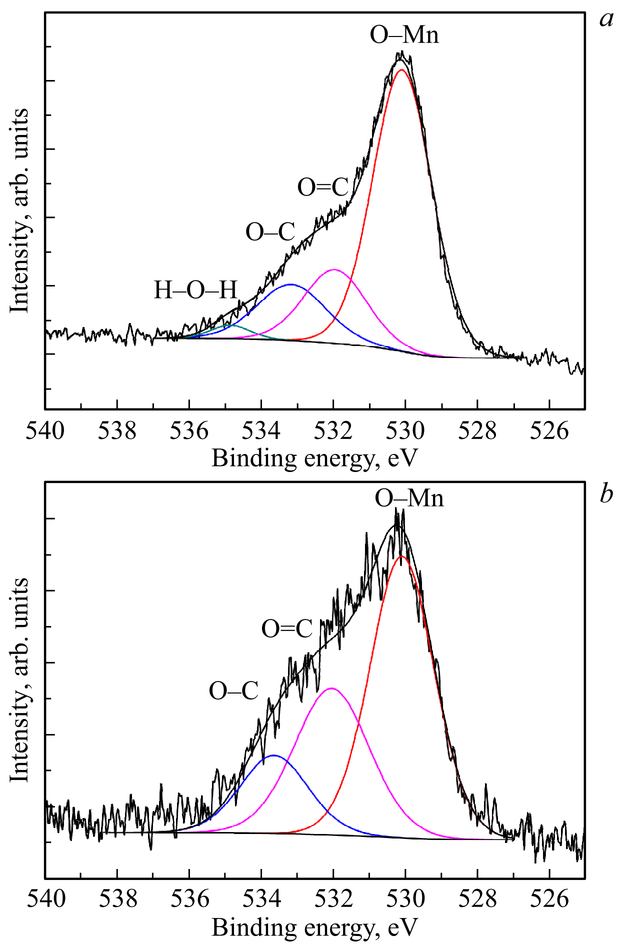

Figure 6. XPS spectra of O1s: *a*) composite MWCNT|MnO$_x$; *b*) MWCNT|MnO$_x$_500.

at half maximum (FWHM) also increases. This indicates the oxidation of the MWCNT during the synthesis of the composite and the associated increase in the degree of defectiveness of the walls of the MWCNT. K2p doublet line is observed in the high-energy region of the spectrum (bond energies 292–298 eV).

The value of the FWHM parameter in the C1s spectrum of the MWCNT|MnO$_x$_500 composite (Figure 5, *c*) is noticeably higher compared to the spectrum of the initial composite. The fitting result indicates an increase in the degree of defectiveness (the relative intensity increases C2). The relative intensity of the components corresponding to carbon-oxygen chemical bonds (C3–C5) also increases significantly. At the same time, the maximum increase is observed for the C3 component corresponding to carbon-oxygen chains with a single chemical bond. It is also important to note that the position of this maximum is shifted to low binding energies (286.1 eV) relative to the position for the spectra of the initial MWCNT and the composite MWCNT|MnO$_x$ (286.5 eV). We believe that this chemical shift may be due to the formation of Mn–O–C-chains at the interface of contact of metal oxide nanoparticles with the surface of the MWCNT.

In the XPS of O1s spectra of the initial composite (Figure 6, *a*), it is observed 4 components that correspond to oxygen in the composition of manganese oxide (∼ 530 eV) [17], C=O- and C–O-links (∼ 532 and ∼ 533 eV respectively) [18,19] are observed in the XPS spectrum of the O1s of the initial composite (Figure 6, *a*), as well as the component (∼ 535 eV) responsible for oxygen states in the composition of adsorbed water [19–21]. There is no component of adsorbed water in the spectrum of the composite after heat treatment (Figure 6, *b*) and there is a noticeable increase in the relative intensity of the components corresponding to C=O and C–O chains. There is a slight shift in the position of their maxima (approximately 0.2 eV) to the region of high bond energies. This may also indicate the formation of chemical bonds at the composite interfaces (Mn–O–C) after heat treatment.

3.3. Analysis of electrochemical characteristics

The CV curve for the MWCNT-based electrode (Figure 7, *a*, curve *1*) has a quasi-rectangular shape characteristic of storing charge in a double electric layer. There are small pseudo-capacitance maxima at the potentials ∼ 0.6 and ∼ 0.5 V at the cathode and anode curves of the CV characteristics, respectively. These maxima may be associated with reversible ORR with the participation of oxygen-containing functional groups which were identified on the surface of the MWCNT using XPS data.

A slight decrease in the area of the CV curves was observed during the initial cycling of the electrodes based on the initial and annealed composites, which, apparently, is due to the irreversible oxidation reactions of Mn(III) to Mn(IV) during interaction with an aqueous electrolyte [22]:

$$Mn_2O_3 + 3H_2O \rightarrow 2MnO_2 + 2H_3O^+ + 2e^-, \qquad (1)$$

$$Mn_3O_4 + 6H_2O \rightarrow 3MnO_2 + 4H_3O^+ + 4e^-. \qquad (2)$$

After several dozen cycles, the CV characteristics stabilized, after which the control measurements presented below were carried out.

The area of the CV curves for composite-based electrodes (Figure 7, curves *2* and *3*) significantly exceeds that for the MWCNT-based electrode. This indicates a higher capacity of composites associated with the reversible interaction of manganese oxide with electrolyte ions [22,23]:

$$MnO_2 + Na^+ + H^+ + 2e^- \leftrightarrow MnOONaH. \qquad (3)$$

A comparative analysis of the CV curves of the composite before and after annealing (Figure 7, curves *2* and *3*) showed that the shape of the MWCNT|MnO curve$_x$_500 is close to quasi-rectangular, whereas in the case of the original composite, the shape of the curve elliptical. This result indicates that the MWCNT|MnO$_x$_500 composite has a better electrochemical behavior compared to the initial composite, whose surface is probably less accessible to

Table 2. Values of the specific discharge capacity of the electrodes at different current densities

	Specific capacitance at different current densities, F/g					
	0.1 A/g	0.2 A/g	0.3 A/g	0.4 A/g	0.5 A/g	1 A/g
MWCNT	18.3	17.5	17.1	16.8	16.1	15.0
MWCNT|MnO$_x$	75.1	73.0	72.5	70.2	61.0	30.2
MWCNT|MnO$_x$_500	88.5	82.0	78.3	74.0	68.8	50.5

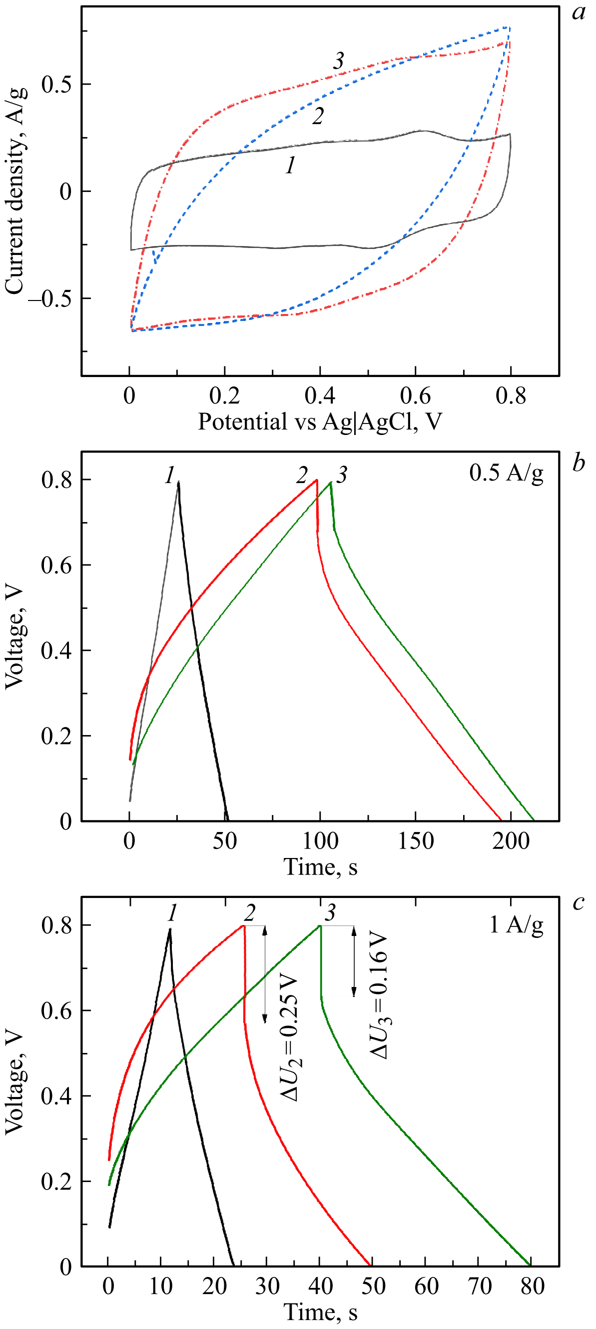

Figure 7. Electrochemical characteristics of electrodes based on MWCNT (*1*), as well as composites MWCNT|MnO$_x$ (*2*) and MWCNT|MnO$_x$_500 (*3*): *a*) — CV curves measured at a potential sweep rate of 10 mV/s; *b*) and *c*) — galvanostatic charge-discharge curves measured at current densities of 0.5 and 1 A/g, respectively.

electrolyte ions or the electrode has a high resistance for the transport of charges through the interfacial interface „manganese oxide—carbon nanotube".

The values of the specific capacitance of the electrodes (presented in Table. 2) were calculated from the results of galvanostatic measurements at different values of the discharge current density (Figure 7, *b* and *c*).

The MWCNT-based electrode has specific capacitance values in the range 18.3—15.0 F/g at discharge current values 0.1—1 A/g. The values of the specific capacitance of the electrode based on the composite MWCNT|MnO$_x$ is ∼ 75—60 F/g at the discharge current density 0.1—0.5 A/g and sharply decreases to ∼ 30 F/g when the current density increases to 1 A/g. The reduction in specific capacity is more than 63%. Whereas for a composite based on MWCNT|MnO$_x$_500, the decrease in specific capacitance is 47% with an increase in the discharge current density from 0.1 to 1 A/g (from ∼ 88 to ∼ 50 F/g).

The range of linear voltage drop in the cell (ΔU) is indicated on the charge-discharge characteristics of the electrodes shown in Figure 7, *c*, for composite electrodes, when the charge mode is switched to discharge mode. This value is directly proportional to the series resistance of the cell, which in this case consists of the resistance of the material and the interface electrode —electrolyte. Apparently, the value of ΔU for the MWCNT|MnO$_x$_500 electrode is significantly lower than the value for the MWCNT|MnO electrode$_x$, which indicates a lower resistance in the case of annealed composite.

The stability of the specific capacitance of the MWCNT|MnO$_x$_500 electrode was evaluated during 500 cycles of galvanostatic charge—discharge at a current density of 0.1 A/g. The result showed the preservation of more than 98% of the initial value.

Based on the set of the data obtained, it can be assumed that the increase in the electrochemical characteristics of the MWCNT|MnO$_x$_500 electrode is attributable to several factors. The transformation of solid layers of manganese oxide into nanoparticles distributed over the surface of the MWCNT, apparently, increases the surface of the electrochemically active metal oxide available to the electrolyte ions. Therefore, despite the decrease in the amount of manganese in the annealed composite, its specific capacity exceeds this value for the initial composite. The increase in the proportion of Mn(III) oxide as a result of annealing, which has a higher resistivity [24] compared to Mn(IV) oxide, also does not negatively affect the properties of the composite. Mn(III) oxides in an aqueous electrolyte can be irreversibly oxidized on the surface of nanoparticles by reactions (1)−(2) and then reversibly interact with electrolyte ions by reaction (3). Based on the XPS data, we can assume that chemically bonded Mn−O−C chains were formed at the composite interfaces during heat treatment. This can reduce the resistance for charge transport and provide more stable capacitive characteristics with an increase in the discharge current density. Taking into account the morphology of the heat-treated composite, it can also be argued that the oxygen-containing groups present (according to the XPS data) on the surface of the MWCNT also participate in reversible ORR when interacting with aqueous electrolytes [25], providing an additional increase in capacity.

4. Conclusion

The structure and electrochemical properties of composites based on MWCNT and manganese oxide formed by precipitation from a solution $KMnO_4$ were studied using a set of experimental methods (SEM, XPS, galvanostatic charge−discharge and CV). It is shown that the proposed synthesis mode makes it possible to form sufficiently uniform layers of manganese oxide up to 25 nm thick on the surface of the MWCNT. Heat treatment of the composite in an inert medium leads to the formation of individual nanoparticles on the surface of the MWCNT with sizes from $\sim 1-20$ nm. The XPS data indicate a high content of oxygen-containing groups on the surface of the MWCNT after annealing of the composite, which suggests an increase in electrochemical activity, as well as the formation of chemical bonds at the interfaces of manganese oxide−MWCNT. The results of galvanostatic analysis indicate a decrease in the electrical resistance of the composite after heat treatment, which confirms the assumption about the chemical interaction of manganese oxide nanoparticles with the surface of the MWCNT. The measurement of the capacitance characteristics showed that the heat treatment of the composite ensures the highest specific capacity: 88.5 F/g at a discharge current density of 0.1 A/g, and preservation of 53% capacity with an increase in the discharge current density by 10 times. Repeated cycling of the electrodes based on the obtained composites showed high stability of their electrochemical characteristics. The results obtained in this work can be used in the development of effective materials and electrochemically active additives for the production of supercapacitor electrodes.

Funding

The study was conducted with the support of the Omsk State Technical University Development Program („Priority 2030").

Conflict of interest

The authors declare that they have no conflict of interest.

References

[1] M.E. Şahin, F. Blaabjerg, A. Sangwongwanich. Energies **15**, *3*, 674 (2022).

[2] L. Miao, Z. Song, D. Zhu, L. Li, L. Gan, M. Liu. Mater. Adv. **1**, *5*, 945 (2020).

[3] H.T. Das, S. Dutta, T.E. Balaji, N. Das, P. Das, N. Dheer, R. Kanojia, P. Ahuja, S.K. Ujjain. Chemosensors **10**, *6*, 223 (2022).

[4] J.H. Lehman, M. Terrones, E. Mansfield, K.E. Hurst, V. Meunier. Carbon **49**, *8*, 2581 (2011).

[5] G.B. Pour, H. Ashourifar, L.F. Aval, S. Solaymani. Symmetry **15**, *6*, 1179 (2023).

[6] B. Wei, L. Wang, Q. Miao, Y. Yuan, P. Dong, R. Vajtai, W.D. Fei. Carbon **85**, 249 (2015).

[7] M. Toupin, T. Brousse, D. Bélanger. Chem. Mater. **16**, *16*, 3184 (2004).

[8] S.J. Uke, V.P. Akhare, D.R. Bambole, A.B. Bodade, G.N. Chaudhari. Front. Mater. **4**, *21*, 1 (2017).

[9] A. Usoltseva, V. Kuznetsov, N. Rudina, E. Moroz, M. Haluska, S. Roth. Phys. Status Solidi B **244**, *11*, 3920 (2007).

[10] V.L. Kuznetsov, D.V. Krasnikov, A.N. Schmakov, K.V. Elumeeva. Phys. Status Solidi B **249**, *12*, 2390 (2012).

[11] M.C. Biesinger, B.P. Payne, A.P. Grosvenor, L.W.M. Lau, A.R. Gerson, R.S.C. Smart. Appl. Surf. Sci. **257**, *7*, 2717 (2011).

[12] P.M. Korusenko, S.N. Nesov. Appl. Sci. **12**, *24*, 12827 (2022).

[13] F. Zeng, Y. Pan, Y. Yang, Q. Li, G. Li, Z. Hou, G. Gu. Electrochim. Acta **196**, 587 (2016).

[14] X. Chen, X. Wang, D. Fang. Fullerenes, Nanotubes. Carbon Nanostruct. **28**, *12*, 1048 (2020).

[15] C.H. Jung, J.Y. Sohn, H.S. Kim, I.T. Hwang, H.J. Lee, J. Shin, J.H. Choi. Appl. Surf. Sci. **439**, 968 (2018).

[16] C. Xu, X. Shi, A. Ji, L. Shi, C. Zhou, Y. Cui. PLoS One **10**, *12*, e0144842 (2015).

[17] R. Cestaro, P. Schweizer, L. Philippe, X. Maeder, A. Serrá. Appl. Surf. Sci. **580**, 152289 (2022).

[18] J.V. Rojas, M. Toro-Gonzalez, M.C. Molina-Higgins, C.E. Castano. Mater. Sci. Eng. B **205**, 28 (2016).

[19] Y. Lei, G. Gao, W. Liu, T. Liu, Y. Yin. Appl. Surf. Sci. **317**, 49 (2014).

[20] H. Ouici, M. Tourabi, O. Benali, C. Selles, M. Traisnel, C. Jama, F. Bentiss, R. Salghi. J. Mater. Environ. Sci. **7**, *8*, 2971 (2016).

[21] M. Pipíška, E.K. Krajcíková, M. Hvostik, V. Friíták, L. Duriška, I. Cernicková, M. Kanuchová, P. Conte, G. Soja. Mater. **15**, *4*, 1492 (2022).

[22] Z.J. Han, D.H. Seo, S. Yick, J.H. Chen, K. Ostrikov. NPG Asia Mater. **6**, *10*, e140 (2014).

[23] M. Huang, F. Li, F. Dong, Y.X. Zhang, L.L. Zhang. J. Mater. Chem. A **3**, *43*, 21380 (2015).

[24] A.L. Pergament, V.P. Malinenko, L.A. Aleshina, V.V. Kolchigin. Phys. Solid State **54**, *12*, 2486 (2012).

[25] Yu.M. Volfkovich. Elektrokhimiya **57**, *4*, 197 (2021). (in Russian).

Translated by A.Akhtyamov